



Multiple block structure-preserving reduced order modeling of interconnect circuits[☆]

Ning Mi, Sheldon X.-D. Tan^{*}, Boyuan Yan

Department of Electrical Engineering, University of California, Riverside, California 92521, USA

ARTICLE INFO

Article history:

Received 8 October 2007

Received in revised form

20 April 2008

Accepted 25 April 2008

Keywords:

Model order reduction

Structure preserving

Interconnect modeling

ABSTRACT

In this paper, we propose a generalized multiple-block structure-preserving reduced order interconnect macromodeling method (BSPRIM). Our approach extends the structure-preserving model order reduction (MOR) method SPRIM [R.W. Freund, SPRIM: structure-preserving reduced-order interconnect macromodeling, in: Proceedings of International Conference on Computer Aided Design (ICCAD), 2004, pp. 80–87] into more general block forms. We first show how an SPRIM-like structure-preserving MOR method can be extended to deal with admittance RLC circuit matrices and show that the $2q$ moments are still matched and symmetry is preserved. Then we present the new BSPRIM method to deal with more circuit partitions for linear dynamic circuits formulated in impedance and admittance forms. The reduced models by BSPRIM will still match the $2q$ moments and preserve the circuit structure properties like symmetry as SPRIM does. We also show that BSPRIM can build the compact models with similar size and accuracy of that produced by traditional projection based methods but using less computation costs. Experimental results show that BSPRIM outperforms SPRIM in terms of accuracy with more partitions and outperforms PRIMA with less CPU times for generating the same accurate models.

© 2008 Elsevier B.V. All rights reserved.

1. Introduction

Compact modeling of passive RLC interconnect networks has been an research intensive area in the past decade due to increasing signal integrity effects and increasing design complexity in current system on a chip (SoC) design [3]. Reducing many parasitic RLC circuits by equivalent compact models in higher level simulation can significantly speedup the simulation and verification process in nanometer VLSI designs.

The most widely used method is based on Krylov subspace methods [4–10]. Krylov subspace method was introduced for interconnect modeling by asymptotic waveform evaluation (AWE) algorithm [4] where explicit moment matching was used to compute dominant poles at low frequency. Pade via Lanczos (PVL) [5], Arnoldi transformation method [6] improved the numerical stability of AWE, congruence transformation method [7] and PRIMA [8] can further produce passive models. However, reduced circuit matrices by PRIMA are larger than direct pole matching (having more poles than necessary) [9,11] and PRIMA does not

preserve certain important circuit structure properties like reciprocity.

Recently, a structure-preserving model (SPRIM) reduction is proposed in [1]. This approach partitions the state matrix in the MNA (modified nodal analysis) form into a natural 2×2 block matrices, i.e. conductance, capacitance, inductance, and adjacent matrices. Accordingly the projection matrix is partitioned. As a result, SPRIM matches the twice moments of the models by using the projection matrix given by PRIMA. The reduced models also preserve the structure properties of the original models like symmetry (reciprocity). This idea has been extended to deal with the more partitions by block structure-preserving model order reduction (BSMOR) [12] to further exploit the regularity of the many parasitic networks. It was shown that by introducing more partitions, more poles can be matched on transformed circuit matrices, which lead to more accurate order reduced models [13].

However, BSMOR method simply introduce more partitions/blocks, it does not truly preserve the circuit structures for general RLC circuits for different input sources (voltages or currents). The reduced model does not match the $2q$ moments of the original models as SPRIM does.

In this paper, we show theoretically that the SPRIM order reduction can be applied to RLC admittance matrices, which are driven by the voltage sources. Then we propose a general block structure-preserving reduced order modeling of interconnects (BSPRIM), which generalizes the SPRIM method [1] by considering

[☆] Some preliminary results of this paper appeared in *IEEE Proc. Int. Symposium. on Quality Electronic Design (ISQED'07)* [2]. This work is funded in part by NSF awards under Grant nos. CCF-0448534 and OISE-0623038, and in part by UC MICRO awards #06-252 via Cadence Design System Inc.

^{*} Corresponding author.

E-mail address: stan@ee.ucr.edu (S.X.-D. Tan).

more partitions. We then study the matrix partitioning for both impedance matrices and admittance matrices separately and show that the reduced models will still match the $2q$ moments of the original circuits and the circuit structures like symmetry, sparsity can be preserved as well.

We also show that by increasing the number of partitions, we can obtain more accurate models at expense of larger model sizes. As a result, we can simply build more accurate models by increasing partitioning number with almost no additional computational costs. This is in contrast with the traditional projection based methods, where accuracy increase can only be obtained by computing more moments, thus increasing the computational costs. Our experimental results confirm the observations.

We notice a similar work published by Freund [14],¹ which presented the structure-preserving MOR of second-order linear dynamic systems and generalized the idea to the higher order linear dynamic systems. It proved that if the system is so-called Hermitian, then the $2q$ moments will still be matched. But this proposed method do not extend to RLC circuits driven by voltage sources, which is typically models for interconnect circuits without grounded resistors. In other words, those interconnect models cannot be driven by current sources.

However, there are some major differences between the proposed work and that in [14]. First, in our paper, we focus on the partitioning of an RLC network into multiple sub-circuits and perform the block structure-preserving reduction instead of higher order linear dynamic systems. Mathematically these two problems are very similar and so do the results. But the proposed BSPRIM method has more observations: by using more partitions, we can obtain more accurate reduced models (although at the cost of large model sizes). However, theoretical study of this problem still remain a challenging problem, we can intuitively explain this by using localized moment matching concept in Section 4.2. The partitioning strategy can be used to reduce the reduction costs for achieving the same accurate models as shown in the experimental part. Our observation is also confirmed by the recent work [13].

Second, we show from a practical RLC circuit perspective that when the inputs to the circuits are driven by voltage sources at the same time, the $2q$ moment matching still hold, this has not been done in [14]. Also the proof of this cases is different from the case for current sources. For general n -block cases, our proof is also different from the proof for high-order differential equations in [14] although the two proofs follow the similar spirit.

The rest of the paper is organized as follows. We review the SPRIM order reduction in Section 2. Then we present the new method to extend SPRIM to deal with admittance matrix with voltage sources in Section 3. After this we present our BSPRIM method in Section 4, where we show that the structure preserving can be extended to $n \times n$ cases for both impedance and admittance matrices and that the $2q$ moments still are matched and symmetric property is preserved. We present the experimental results and discussions in Section 5, and conclude the paper in Section 6. Proofs of some key theorems will be included in the Appendix.

2. Block SPRIM reduction

In this section, we review the structure-preserving projection based MOR method SPRIM and the important results of SPRIM method.

2.1. Preliminary

Consider a modified nodal formulation (MNA) of the RLC circuit equation in the frequency domain:

$$\begin{aligned} \mathcal{G}x(s) + s\mathcal{C}x(s) &= \mathcal{B}i_p(s), \\ v_p(s) &= \mathcal{B}^T x(s), \end{aligned} \quad (1)$$

where $x(s)$ is the state variable vector, \mathcal{G} and \mathcal{C} ($\in \mathbb{R}^{N \times N}$) are state matrices. \mathcal{B} ($\in \mathbb{R}^{N \times n_p}$) is

$$\mathcal{B} = [\mathcal{B}_1^T \quad 0]^T, \quad (2)$$

a port incident matrix. We assume that we have only current sources indicated by $i_p(s)$ first. Eliminating $x(s)$ in Eq. (1) gives

$$\begin{aligned} v_p(s) &= H(s)i_p(s), \\ H(s) &= \mathcal{B}^T(\mathcal{G} + s\mathcal{C})^{-1}\mathcal{B}, \end{aligned} \quad (3)$$

where $H(s)$ is a multiple-input multiple-output (MIMO) impedance transfer function. PRIMA finds a projection matrix V ($\in \mathbb{R}^{N \times q}$) such that its columns span the q -th block Krylov subspace $\mathcal{K}(\mathcal{A}, \mathcal{B}, q)$, i.e.

$$\text{span}V = \mathcal{K}(\mathcal{A}, \mathcal{B}, q), \quad (4)$$

where $\mathcal{A} = (\mathcal{G} + s_0\mathcal{C})^{-1}\mathcal{C}$, $\mathcal{B} = (\mathcal{G} + s_0\mathcal{C})^{-1}\mathcal{B}$, and s_0 is the expansion point that ensures $\mathcal{G} + s_0\mathcal{C}$ is nonsingular. The resulting reduced transfer function is

$$\tilde{H}(s) = \tilde{\mathcal{B}}^T(\tilde{\mathcal{G}} + s\tilde{\mathcal{C}})^{-1}\tilde{\mathcal{B}}, \quad (5)$$

where

$$\tilde{\mathcal{G}} = V^T\mathcal{G}V, \quad \tilde{\mathcal{C}} = V^T\mathcal{C}V, \quad \tilde{\mathcal{B}} = V^T\mathcal{B} \quad (6)$$

has the identical expanded first q -th (block) moments of the original transfer function $H(s)$. It is called as the *Grimme's projection theorem* [15]. Note that $\tilde{\mathcal{G}}, \tilde{\mathcal{C}}$ are $\in \mathbb{R}^{q \times q}$, and $\tilde{\mathcal{B}}$ is $\in \mathbb{R}^{q \times n_p}$.

The PRIMA-like MOR method cannot preserve the structure of the original circuit model. This reflects in the fact that if impedance transfer function $H(s)$ is symmetric, the reduced transfer function $\tilde{H}(s)$ is no longer symmetric. Also the reduced matrices $\tilde{\mathcal{G}}, \tilde{\mathcal{C}}$ become very dense or are full matrices.

2.2. The SPRIM method

In [1], a structure-preserving reduced model order reduction technique, SPRIM, was proposed. The primary observation is that impedance transfer function of RLC circuit $H(s)$ is symmetric. By using a split projection matrix, the structure information relevant to the passive and symmetric properties of the original circuit matrices is still preserved. As a result, the reduced transfer function $\tilde{H}(s)$ is still symmetric.

This structure-preserving MOR was made possible by the observation that instead of using the Krylov subspace $\mathcal{K}(\mathcal{A}, \mathcal{B}, q)$ for the projection matrix \tilde{V} , one can use any projection matrix such that the space spanned by the columns in \tilde{V} contains the q -th block Krylov subspace, i.e.

$$\mathcal{K}(\mathcal{A}, \mathcal{B}, q) \subseteq \tilde{V}. \quad (7)$$

SPRIM starts with the 2×2 structured MNA circuit matrices in the following form:

$$\mathcal{G} = \begin{bmatrix} G & A^T \\ -A & 0 \end{bmatrix}, \quad \mathcal{C} = \begin{bmatrix} C & 0 \\ 0 & L \end{bmatrix}, \quad \mathcal{B} = \begin{bmatrix} B_1 \\ 0 \end{bmatrix}, \quad (8)$$

where $G(\in \mathbb{R}^{n_1 \times n_1})$, $C(\in \mathbb{R}^{n_1 \times n_1})$, $L(\in \mathbb{R}^{n_2 \times n_2})$ are conductance, capacitance, and inductance matrix, and $(A \in \mathbb{R}^{n_2 \times n_1})$ is the adjacent matrix indicating the branch currents inside inductors. Note that $n_1 + n_2 = N$.

¹ We were not aware of this work when our research work was performed.

Therefore, a structured projection vector \tilde{V} is constructed by partitioning the projection vector V obtained from the q -th PRIMA iteration

$$V = \begin{bmatrix} V_1 \\ V_2 \end{bmatrix} \rightarrow \tilde{V} = \begin{bmatrix} V_1 & 0 \\ 0 & V_2 \end{bmatrix}, \quad (9)$$

where V_1 is $\in R^{n_1 \times q}$, V_2 is $\in R^{n_2 \times q}$, and hence \tilde{V} is $\in R^{N \times 2q}$. As a result, the number of columns in \tilde{V} is twice as that in V . Accordingly the new reduced state matrices are

$$\tilde{\mathcal{G}} = \begin{bmatrix} \tilde{G} & \tilde{A}^T \\ -\tilde{A} & 0 \end{bmatrix}, \quad \tilde{\mathcal{C}} = \begin{bmatrix} \tilde{C} & 0 \\ 0 & \tilde{L} \end{bmatrix}, \quad (10)$$

where $\tilde{G} = V_1^T G V_1$, $\tilde{A} = V_2^T A V_1$, $\tilde{C} = V_1^T C V_1$, and $\tilde{L} = V_2^T L V_2$. Similarly, the size of $\tilde{\mathcal{G}}$, $\tilde{\mathcal{C}}$ ($\in R^{2q \times 2q}$), and $\tilde{\mathcal{B}}$ ($\in R^{2q \times n_p}$) is twice as that of \mathcal{G} , \mathcal{C} , and \mathcal{B} reduced by using V .

In addition to the preservation of the structure of MNA matrices, an important benefit of SPRIM is that the reduced models will match $2q$ block moments given q -th block Krylov subspace $\mathcal{K}(\mathcal{A}, \mathcal{B}, q)$. The $2q$ matching property of SPRIM mainly are owing to the fact that both the original impedance and reduced impedance transfer functions are symmetric when structure is preserved. When symmetric transfer functions are reduced, $2q$ moments are matched because of the use of two Krylov spaces (the input and output Krylov subspaces, which are same in this case) [10].

However, the SPRIM method [1] only gives the structure-preserving MOR on the impedance matrices with current input sources. We show in the following section that admittance circuit matrices, which are driven only by voltage sources can also be reduced in a structure-preserving way.

3. Structure preserving for admittance transfer function matrices

In this section, we show that for admittance transfer functions, by properly partitioning the circuit matrices and splitting the projection matrix, we can still preserve the structure of the admittance circuit matrices and achieve the $2q$ moment matching result.

3.1. Circuit structure partitioning

For RCL circuit with voltage sources, the resulting MNA equation is written as

$$\mathcal{G}X + \mathcal{C} \frac{dx}{dt} = \mathcal{B}u_t(t), \quad (11)$$

where

$$\mathcal{G} = \begin{bmatrix} E_g^T G E_g & E_l^T & E_v^T \\ -E_l & 0 & 0 \\ -E_v & 0 & 0 \end{bmatrix}, \quad \mathcal{C} = \begin{bmatrix} E_c^T C E_c & 0 & 0 \\ 0 & L & 0 \\ 0 & 0 & 0 \end{bmatrix},$$

$$\mathcal{B} = \begin{bmatrix} 0 \\ 0 \\ E_v^T \end{bmatrix}, \quad (12)$$

where E_x is the incident (adjacency) submatrix for corresponding type of branches in the circuit and $u_t(t)$ is the vector of input voltage sources. The transfer admittance function becomes

$$Y(s) = \mathcal{B}^T (\mathcal{G} + s\mathcal{C})^{-1} \mathcal{B}. \quad (13)$$

As a result, we can still partition the circuit matrices into a 2×2 form as follows:

$$\mathcal{G} = \begin{bmatrix} G_1 & G_2^T \\ -G_2 & 0 \end{bmatrix}, \quad \mathcal{C} = \begin{bmatrix} C_1 & 0 \\ 0 & C_2 \end{bmatrix}, \quad \mathcal{B} = \begin{bmatrix} 0 \\ B_2 \end{bmatrix}, \quad (14)$$

where G_1 and C_1 , G_2 and C_2 are defined as

$$G_1 = E_g^T G E_g, \quad G_2 = \begin{bmatrix} -E_l \\ -E_v \end{bmatrix},$$

$$C_1 = E_c^T C E_c, \quad C_2 = \begin{bmatrix} L & 0 \\ 0 & 0 \end{bmatrix},$$

$$B_2 = \begin{bmatrix} 0 \\ E_v^T \end{bmatrix}. \quad (15)$$

Meanwhile, subblock matrices G_1, C_1, C_2 are positive semidefinite. i.e. they satisfy

$$G_1 \succcurlyeq 0, \quad C_1 \succcurlyeq 0, \quad C_2 \succcurlyeq 0. \quad (16)$$

Note that by comparing (8) and (14), one finds that the major difference between impedance and admittance is that the position matrices \mathcal{B} are different. It turns out that this difference will not affect the $2q$ moment matching property by using structure-preserving reduction as shown in Theorem 1.

After getting V from q -th PRIMA, we obtain \tilde{V} by partitioning V conformly according to the size of \mathcal{G} , \mathcal{C} , and \mathcal{B} ,

$$V = \begin{bmatrix} V_1 \\ V_2 \end{bmatrix} \rightarrow \tilde{V} = \begin{bmatrix} V_1 & 0 \\ 0 & V_2 \end{bmatrix}. \quad (17)$$

Here the rows of V_1, V_2 equal to the rows of G_1, G_2 , respectively. The new reduced matrix can be obtained by

$$\tilde{\mathcal{G}} = \tilde{V}^T \mathcal{G} \tilde{V} = \begin{bmatrix} \tilde{G}_1 & \tilde{G}_2^T \\ -\tilde{G}_2 & 0 \end{bmatrix}, \quad \tilde{\mathcal{C}} = \tilde{V}^T \mathcal{C} \tilde{V} = \begin{bmatrix} \tilde{C}_1 & 0 \\ 0 & \tilde{C}_2 \end{bmatrix},$$

$$\tilde{\mathcal{B}} = \tilde{V}^T \mathcal{B} = \begin{bmatrix} 0 \\ \tilde{B}_2 \end{bmatrix}. \quad (18)$$

The corresponding transfer function is

$$\tilde{Y}(s) = \tilde{\mathcal{B}}^T (\tilde{\mathcal{G}} + s\tilde{\mathcal{C}})^{-1} \tilde{\mathcal{B}}. \quad (19)$$

It can be proved that the reduced admittance matrix $\tilde{Y}(s)$ is still symmetric. So reciprocity property is still preserved.

3.2. Re-orthonormalization of split projection matrix

For the projection matrix $V \in R^{N \times q}$ in (17), its rank should be q (assuming $N > q$). After the 2-way splitting operation in (17), the rank of \tilde{V} , however, may not be $2q$ and it typically is less than $2q$. The reason is that after splitting operations, some columns may become linear dependent. Also the columns in \tilde{V} are no longer orthogonal to each other, i.e.

$$\tilde{V}^T \tilde{V} \neq I$$

which is required for numerical stability in the reduction process. The orthogonalization process is important for the projection based reduction method. Without it, the reduced system may have redundant information. For instance, for a matrix A , let λ_i be one of its eigenvalues with x_i being the corresponding eigenvector, i.e. $Ax_i = \lambda_i x_i$. If we use nonorthogonal matrix $X = [x_i, x_i]$ as the projection matrix, then $\tilde{A} = X^T A X = \text{diag}(\lambda_i, \lambda_i)$. So the resulting reduced matrix has two identical eigenvalues. Practically, the resulting matrix will be larger than the one reduced by the orthogonal projection matrix. Also if we do not use an orthogonal projection matrix, the reduced matrix may even have positive poles.

To mitigate this problem, we re-orthonormalize each subblock in \tilde{V} and obtain the new split projection matrix \tilde{T}

$$\tilde{T} = \begin{bmatrix} \text{orth}(V_1) & 0 \\ 0 & \text{orth}(V_2) \end{bmatrix}, \quad (20)$$

where $\text{orth}(X)$ means making the orthonormal basis for matrix X . As a result, we may end up with less columns in \tilde{T} than in \tilde{V} , which leads to smaller sizes of the reduced models. Also \tilde{T} becomes orthogonal again

$$\tilde{T}^T \tilde{T} = I. \quad (21)$$

We also remark that the re-orthonormalization process does not change the subspace of \tilde{V} and the moment matching property of \tilde{V} is also valid for \tilde{T} . But experimental results show that the re-orthonormalization can always lead to the same or more accurate reduced models owing to the improved numerical stability.

3.3. Structure-preserving properties

The proposed 2×2 structure-preserving MOR method for admittance transfer function matrices has the similar properties as the SPRIM for RCL circuits containing current sources. As a result, the reduced transfer function $\tilde{Y}(s)$ is still symmetric and reciprocal property is preserved.

The moment-matching property can be stated as follows:

Theorem 1. *Choosing $s_0 \in \mathfrak{R}$. Let $n = m_1 + m_2 + \dots + m_q$ and let \tilde{V} be the matrix used in the proposed algorithm. Therefore, the first $2q$ moments in the expansions of $Y(s)$ in (13) and the projected model $\tilde{Y}_n(s)$ in (19) about s_0 are identical:*

$$Y(s) = \tilde{Y}_n(s) + o((s - s_0)^{2q}). \quad (22)$$

The proof sketch of the theorem is given in the Appendix. Regarding the passivity, it can be easily proved that the reduced admittance transfer function in (19) is positive real and thus passive.

For an RLC circuit in MNA formulation, if it is driven by both current and voltage sources, the input position matrix \mathcal{B} becomes

$$\mathcal{B} = [B_1^T \quad B_2^T]^T. \quad (23)$$

The resulting transfer function is a hybrid function matrix function, which is no longer symmetric in general. Neither is the reduced model. The $2q$ moment matching property, however, may still hold subject to future investigation.

4. General block SPRIM order reduction method

Structure-preserving MOR methods like SPRIM essentially are based on a 2×2 partitioning of the state matrices. To be more general than structure-preserving algorithm for either impedance form or admittance form, we can make more partitions based on the algorithm mentioned before in order to get relatively lower order model than the original order. In this section, we will introduce this multiple-block SPRIM order reduction, method, called *BSPRIM*, for both impedance and admittance transfer functions.

We show that by increasing the partition number or block number, we can obtain more accurate reduced models. BSPRIM can still match the $2q$ moments of the original transfer impedance or admittance transfer functions, which is in contrast to the recent work [12]. The BSPRIM method leads to localized model order reduction on sub-circuits and can preserve the sparsity of the original circuit matrices.

4.1. Block structure-preserving MOR for impedance function matrices

For impedance transfer function matrices, to partition the original circuits into m blocks (nodes disjoint partitions), we need to partition the MNA circuit into $(m + 1)$ blocks for \mathcal{G} , \mathcal{C} , and \mathcal{B} , respectively, to preserve the structure relevant to the symmetric and moment matching properties as shown below:

$$\mathcal{G} = \begin{bmatrix} G_1 & G_2^T \\ -G_2 & 0 \end{bmatrix},$$

where G_1, G_2 are given as

$$G_1 = \begin{bmatrix} \mathcal{G}_{1,1(n_1 \times n)} & \dots & \mathcal{G}_{1,m-1(n_1 \times n)} & \mathcal{G}_{1,m(n_1 \times n)} \\ \mathcal{G}_{2,1(n_2 \times n)} & \dots & \mathcal{G}_{2,m-1(n_2 \times n)} & \mathcal{G}_{2,m(n_2 \times n)} \\ \vdots & \ddots & \vdots & \vdots \\ \mathcal{G}_{m,1(n_m \times n)} & \dots & \mathcal{G}_{m,m(n_m \times n)} & \mathcal{G}_{m,m(n_m \times n)} \end{bmatrix}, \quad (24)$$

$$G_2 = [\mathcal{G}_{m+1,1(n_{m+1} \times n)}, \mathcal{G}_{m+1,2(n_{m+1} \times n)}, \dots, \mathcal{G}_{m+1,m(n_{m+1} \times n)}]$$

and each block has the size n_k ($\sum_{k=1}^{m+1} n_k = N$). ($n_x \times n$) stands for the matrix size of $\mathcal{G}_{ij(n_x \times n)}$. Then, \mathcal{C} matrix becomes

$$\mathcal{C} = \begin{bmatrix} C_1 & 0 \\ 0 & C_2 \end{bmatrix}.$$

In \mathcal{C} , C_1 and C_2 represent

$$C_1 = \begin{bmatrix} \mathcal{C}_{1,1(n_1 \times n)} & 0 & \dots & 0 \\ 0 & \mathcal{C}_{2,2(n_2 \times n)} & \dots & 0 \\ \vdots & \vdots & \ddots & \vdots \\ 0 & 0 & \dots & \mathcal{C}_{m,m(n_m \times n)} \end{bmatrix}, \quad (25)$$

$$C_2 = C_{m,m(n_{m+1} \times n)}.$$

The position matrix \mathcal{B} now is partitioned conformly

$$\mathcal{B} = [B_1, 0], \quad B_1 = [B_{1(n_1 \times n)}, B_{2(n_2 \times n)}, \dots, B_{m(n_m \times n)}]^T, \quad (26)$$

where ($n_x \times n$) stands for the matrix size of $\mathcal{C}_{ij(n_x \times n)}$ and $B_{1(n_1 \times n)}$. Therefore, the reduced state matrices can be obtained as mentioned in Section 2.

The projection matrix \hat{V} , according to the partition of \mathcal{G} and \mathcal{C} , can be obtained by $(m + 1)$ -way splitting of the projection matrix V obtained from the PRIMA:

$$V = \begin{bmatrix} V_{1(n_1 \times n)} \\ V_{2(n_2 \times n)} \\ \vdots \\ V_{m+1(n_{m+1} \times n)} \end{bmatrix} \rightarrow \hat{V} = \begin{bmatrix} V_{1(n_1 \times n)} & 0 & \dots & 0 \\ 0 & V_{2(n_2 \times n)} & \dots & 0 \\ \vdots & \vdots & \ddots & 0 \\ 0 & 0 & \dots & V_{m+1(n_{m+1} \times n)} \end{bmatrix}. \quad (27)$$

As a result,

$$\hat{\mathcal{G}}_n = \hat{V}^T \mathcal{G} \hat{V}, \quad \hat{\mathcal{C}}_n = \hat{V}^T \mathcal{C} \hat{V}, \quad \hat{\mathcal{B}}_n = \hat{V}^T \mathcal{B}. \quad (28)$$

More specifically, every block in $\hat{\mathcal{G}}$, $\hat{\mathcal{C}}$, and $\hat{\mathcal{B}}$ can be expressed as

$$\hat{\mathcal{G}}_{ij} = V_i^T \mathcal{G}_{ij} V_j, \quad \hat{\mathcal{C}}_{ij} = V_i^T \mathcal{C}_{ij} V_j, \quad \hat{\mathcal{B}}_i = V_i^T \mathcal{B}_i. \quad (29)$$

We remark that for m -way partitioning of the original circuit, we have $(m + 1)$ -way partitioning of the circuit matrices.

With the reduced circuit matrix, we have the reduced-order model with the transfer function:

$$\hat{Z}_n(s) = \hat{\mathcal{B}}^T (\hat{\mathcal{G}} + s\hat{\mathcal{C}})^{-1} \hat{\mathcal{B}}. \quad (30)$$

As a result, we have the following theorem regarding the BSPRIM method:

Theorem 2. *Choosing $s_0 \in \Re$. Let $n = m_1 + m_2 + \dots + m_q$ and let \hat{V}_n be the matrix used in the BSPRIM algorithm from (27). Therefore, the first $2q$ moments in the expansions of the original impedance transfer function Z and the reduced impedance transfer function \hat{Z}_n (30) about s_0 are identical:*

$$Z(s) = \hat{Z}_n(s) + o((s - s_0)^{2q}). \quad (31)$$

The proof sketch of this theorem is in the Appendix. Similar to SPRIM, BSPRIM also preserves the passivity of the reduced models. This is reflected by the fact that both $\hat{\mathcal{G}}$ and $\hat{\mathcal{C}}$ are still positive definite after structure-preserving MOR. We then have the following result regarding the passivity:

Theorem 3. *BSPRIM order reduced impedance model $\hat{Z}_n(s)$ in (31) is passive.*

4.2. Localized moment matching and new way for accuracy improvement

In this subsection, we give some explanation for the observation that by increasing the partition number, the reduced model becomes more accurate while it still matches $2q$ moments. One explanation of better accuracy is that the reduced models match more poles with more partition numbers, which lead to more accurate models as confirmed by our experimental results and the earlier work [12]. We remark that the accuracy increase comes with the increase of the model sizes (and also more nonzero elements in the reduced matrices). This is true for both methods. But our experimental results show that given approximately the same nonzero elements in the reduced models produced by both methods, the accuracies of the two models are similar. As a result, the new approach can simply improve the model accuracy by increasing the partition numbers, with marginal computing costs. This is in contrast to the traditional projection based method where the increase of accuracy has to be obtained by computing more moments, which is more expensive.

The more matched poles can be explained by the concept of *localized moment matching*. We observe that the partitioned projection matrix \hat{V} leads to the localized projection by using partitioned Krylov subspaces as shown by (29). In other words, the block projection matrix \hat{V}_i is used only for matrix blocks $\mathcal{G}_{i,x}$ and $\mathcal{G}_{x,i}$, ($x = 1, \dots, m+1$). Each structured block projection matrix \hat{V}_i will lead to the localized model order reduction for block i , which is represented by $\mathcal{G}_{x,i}$ and $\mathcal{G}_{i,x}$ matrix blocks ($x = 1, \dots, m$). For each block, the maximum order is much smaller than the total order of the whole circuit. As we reduce the block size, thus by increasing the partition number, the matched moments order will get close to the maximum order of each block. Conceivably, if the \hat{V} reaches to the same size as \mathcal{G} and \mathcal{C} with sufficient partition number, all the poles of original systems will be preserved and thus matched since the corresponding congruence transformation becomes similarity transformation (as $\hat{V}^T \hat{V} = I$), which preserves all the system poles.

In summary, by introducing more partitioning number and thus more partitioned Krylov subspaces, one can obtain reduced order models with more accurate for each structure block by using the same Krylov subspace base vectors, or get the same order reduced model (same accuracy) using the smaller Krylov sub-

space. Therefore, BSPRIM provides more flexibility and trade-off between efficiency and model accuracy for reducing linear dynamic system models than the traditional projection based reduction methods like PRIMA.

4.3. Block structure-preserving MOR for admittance function matrices

In this case, we have $(m+1)$ partitioning of the circuit matrices for m -way circuit node partitioning based on the result in Section 3:

$$\mathcal{G} = \begin{bmatrix} G_1 & G_2^T \\ -G_2 & 0 \end{bmatrix}, \quad \mathcal{C} = \begin{bmatrix} C_1 & 0 \\ 0 & C_2 \end{bmatrix}, \quad \mathcal{B} = \begin{bmatrix} 0 \\ B_2 \end{bmatrix}, \quad (32)$$

where G_1 and C_1 have the m -way partitioned block structure as shown in (24) and (25), respectively.

Accordingly, we split the projection matrix V obtained from PRIMA into $m+1$ partitions to preserve the structure of \mathcal{G} , \mathcal{C} , and \mathcal{B} . When splitting V obtained from PRIMA, the number of rows of V_{m+1} should equal to the row number of G_2 , i.e.

$$V = \begin{bmatrix} V_1 \\ \vdots \\ V_m \\ V_{m+1} \end{bmatrix} \rightarrow \hat{V} = \begin{bmatrix} V_1 & 0 & \dots & 0 \\ 0 & \ddots & \dots & 0 \\ \vdots & 0 & V_m & 0 \\ 0 & 0 & 0 & V_{m+1} \end{bmatrix}. \quad (33)$$

The corresponding $\hat{\mathcal{G}}$, $\hat{\mathcal{C}}$, and $\hat{\mathcal{B}}$ are obtained as follows and the structure is preserved.

$$\begin{aligned} \hat{\mathcal{G}}_n &= \hat{V}^T \mathcal{G} \hat{V}, & \hat{\mathcal{C}}_n &= \hat{V}^T \mathcal{C} \hat{V}, & \hat{\mathcal{B}}_n &= \hat{V}^T \mathcal{B}. \\ \hat{\mathcal{G}}_{ij} &= V_i^T \mathcal{G}_{ij} V_j, & \hat{\mathcal{C}}_{ij} &= V_i^T \mathcal{C}_{ij} V_j, & \hat{\mathcal{B}}_i &= V_i^T \mathcal{B}_i. \end{aligned} \quad (34)$$

The transfer function is

$$\hat{Y}_n(s) = \hat{\mathcal{B}}^T (\hat{\mathcal{G}} + s\hat{\mathcal{C}})^{-1} \hat{\mathcal{B}}. \quad (35)$$

It also has the following moment matching properties:

Theorem 4. *Let $s_0 \in \Re$, $n = m_1 + m_2 + \dots + m_q$ and \hat{V} be the matrix used in our proposed algorithm. Therefore, the first $2q$ moments in the expansions of $Y(s)$ and the projected model \hat{Y}_n in (35) about s_0 are identical:*

$$Y(s) = \hat{Y}_n(s) + o((s - s_0)^{2q}). \quad (36)$$

The proof is similar to Theorem 2. Similarly, reduced admittance transfer function models $Y(s)$ by BSPRIM are also passive.

5. Experiment result

The proposed BSPRIM has been implemented in Matlab 7.0 and a number of RLC circuits are used to illustrate effectiveness of the proposed BSPRIM method to reduce circuit matrices formulated in both impedance and admittance forms. We compare the proposed method with PRIMA and SPRIM for different circuits and then show the higher accuracy of the BSPRIM over the two methods. We also show that by increasing the partitioning number, we can build more accurate models, which has the similar accuracy to the models built by PRIMA if they have the similar nonzero elements in the reduced models.

5.1. Comparison results for circuits in impedance forms

The first example is an RLC ladder-like circuit with about 202 nodes, which models the transmission lines. The reduced order of PRIMA is set to $n = 15$ and the number of blocks (partitions) used

in BSPRIM is 4 ($m = 3$) and the reduced order $n = 15$ is used for each block. We observe the transfer function response from the input port two, out port one (z_{12}). In the following, all the responses are real part of the complex transfer function responses in the frequency domain.

Fig. 1 shows the responses of the transfer functions z_{12} of BSPRIM over SPRIM and PRIMA. Fig. 2 is the sparsity comparison among reduced circuit matrices by PRIMA, by BSPRIM and the original circuit.

From Fig. 1, we can see that the reduced model by SPRIM is more accurate than that of PRIMA. While BSPRIM using 4×4

block is much more accurate than SPRIM and PRIMA over higher frequency range (from 30 to 40 GHz).

The matrix sparsity structures are shown in Fig. 2 for this circuit for the reduced models by PRIMA and BSPRIM. We notice that PRIMA produces full dense matrices, while the reduced model by BSPRIM are not full matrices any more. We notice that the reduced matrices by BSPRIM have more nonzero elements than the reduced matrices of PRIMA and even the original matrices. This is not surprising as we use the same reduced order ($n = 15$) for each block in BSPRIM. After the reduction, each reduced matrix block is full sub-matrix. We notice that the reduced C matrix by PRIMA has more number of nonzero elements than that of the original matrix. If we have more partitions, we will see that both reduced matrices (G and C matrices) by BSPRIM will become more sparse.

We will observe later that, if the reduced models by PRIMA and BSPRIM have the similar number of nonzero elements, their accuracies will be similar.

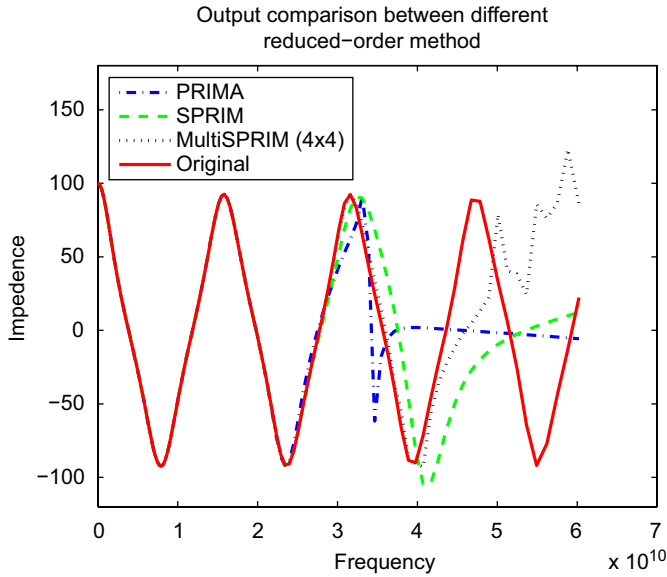


Fig. 1. Accuracy comparison among SPRIM, PRIMA and BSPRIM for impedance form on the circuit with 202 nodes on z_{12} .

5.2. Comparison results for circuits in admittance forms

In the following, we show the experiment results of BSPRIM for circuits in the admittance form on the same circuit with 202 nodes driven now by voltage sources. The reduced order by PRIMA is $n = 15$. We use a 2×2 partition for the BSPRIM and the number of block is 2 ($m = 1$). Fig. 3 shows the accuracy comparison of the proposed algorithm with PRIMA. We still observe the transfer function from the input port two, out port one (y_{12}). From Fig. 3, we can see that the reduced model of BSPRIM is more accurate than that of PRIMA for very high frequency range.

Fig. 4 is the comparison of the sparsity matrix structure of the reduced models by PRIMA, BSPRIM and that of the original circuit used above. We can see the sparsity and structure-preserving characteristic of our BSPRIM.

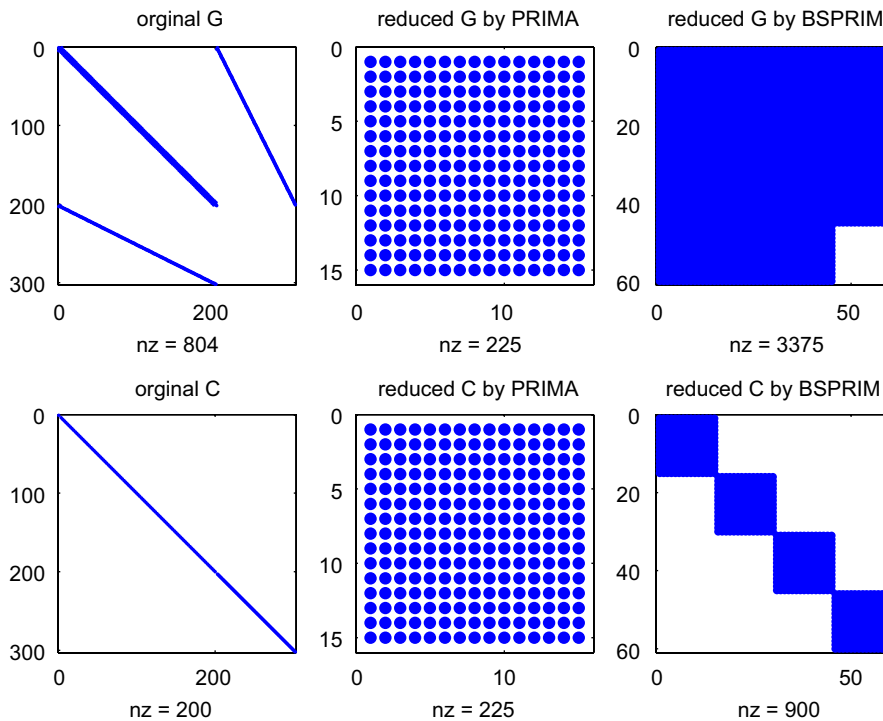


Fig. 2. Structures of the reduced matrices of PRIMA and BSPRIM on the circuit with 202 nodes.

5.3. Study of the re-orthonormalization process

To study the effects of the re-orthonormalization process, we choose a second RLC interconnect circuit with 602 nodes, which is driven by voltage sources only and the transfer function is admittance.

For this circuit, we have a 15×15 partition of the original circuit. The reduced order of PRIMA is $n = 15$ and the number of blocks equals to 15 ($m = 14$). We still observe the admittance from the input port two, output port one (y_{12}). Fig. 5 shows the better accuracy of BSPRIM over the algorithm mentioned in Section 3 and PRIMA. From Fig. 5, we can see that BSPRIM with the re-orthonormalization is much more accurate than BSPRIM without the re-orthonormalization. Also, after the re-orthonormalization, the dimension of the reduced-order model is reduced from

225 to 221. So we generate smaller reduced models while achieving better accuracy at the same time. Fig. 6 shows the matrix sparsity of the original circuit, reduced matrices by PRIMA and BSPRIM.

We remark that in this case, the reduced circuit matrices by BSPRIM are very sparse although they have more nonzero elements than the original circuits. But the reduced model is much more accurate than that of PRIMA over large frequency range from 7 to 20 GHz.

5.4. Relationship between accuracy and nonzero element counts

Now, we show that the new approach can deliver reduced models that are as accurate as that of PRIMA with less or similar

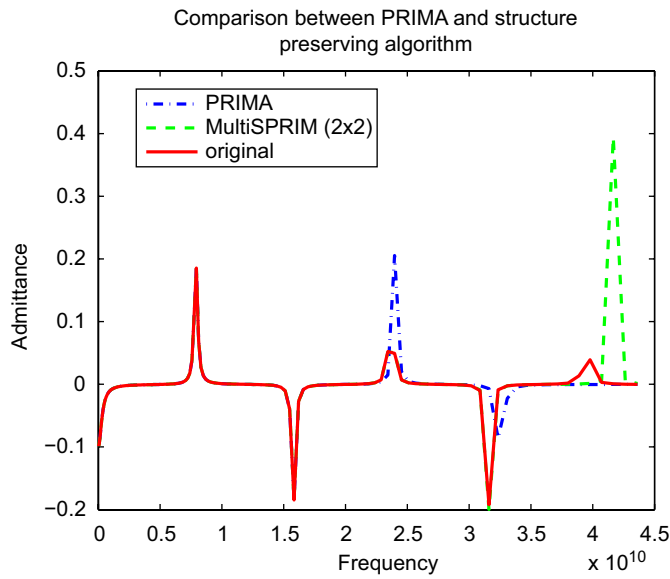


Fig. 3. Accuracy comparison between PRIMA and BSPRIM with admittance form on the circuit with 202 nodes on y_{12} .

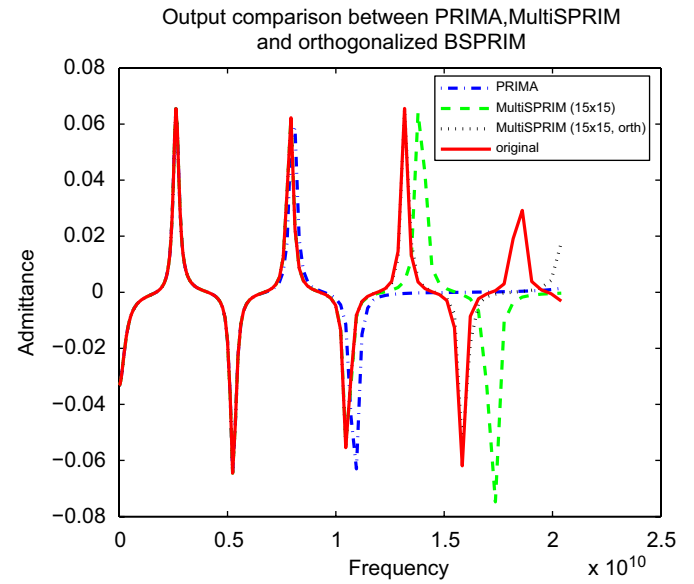


Fig. 5. Comparison between PRIMA and BSPRIM with and without re-orthonormalization on the circuit with 602 nodes in admittance form on y_{12} .

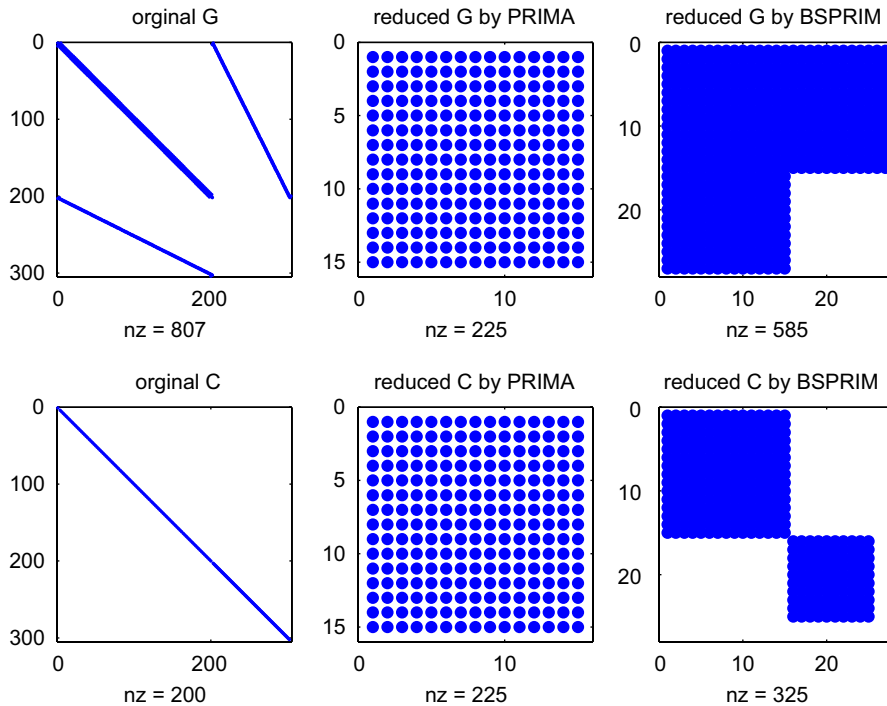


Fig. 4. Structures of the reduced matrices by PRIMA and BSPRIM on the circuit with 202 nodes.

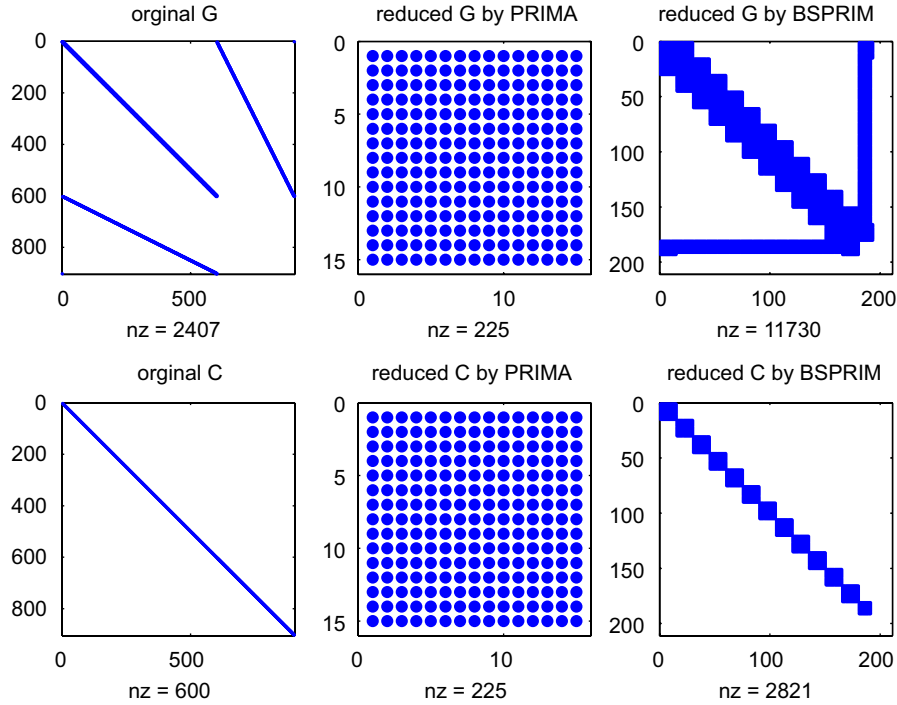


Fig. 6. Structures of the reduced matrices of PRIMA and BSPRIM with re-orthonormalization on the circuit with 602 nodes.

number of nonzero elements. At the same time, the sparsity and block structure inherent to RLC circuits can be preserved.

The example is an RLC circuit with 824 nodes with voltage sources as inputs. First, we partition the projection matrix into two parts and BSPRIM will result in a reduced model of order 25. Compared with the reduced model of order 20 by PRIMA, the reduced model has same accuracy up to 30 GHz as shown in Fig. 7. Here, we observe admittance from the port with input port two and out port one, i.e. y_{12} . However, the reduced model by PRIMA has 800 nonzero elements for both reduced G and C matrices while BSPRIM has about 760 nonzero elements as shown in Fig. 8.

BSPRIM can reduce the computation cost in both modeling process and simulation process. In this example, BSPRIM only needs to compute half of the Krylov subspace vectors as PRIMA does. As a result, the modeling time for BSPRIM is 0.96 s, which is in contrast with 1.64 s for PRIMA.

In addition, if we partition the projection matrix into four parts with less moment order ($q = 7$), the resulted BSPRIM reduced model of order 30 will still have about the same number of nonzero elements as the PRIMA reduced model of order 20 with similar accuracy as shown in Figs. 9 and 10. In Fig. 9, we still observe the admittance from input port two and output port one (y_{12}). While in this example, BSPRIM only uses 0.75 s to perform the reduction, which is less than the half of the time (1.64) used by PRIMA.

As a result, we observe that if the total numbers of nonzero elements are similar, the reduced models produced by PRIMA and BSPRIM are similar in accuracy while BSPRIM is faster than PRIMA.

Last but not least, we show that if we increase the partitioning number and keep the reduced order the same for each sub-block, we can continue to improve the accuracy of the reduced models. As shown in Fig. 11, we partition the projection matrix with different blocks: $3 \times 3, 4 \times 4, 5 \times 5, 6 \times 6$, respectively, which result in the reduced models of sizes 12, 20, 28, 36, respectively, with the obviously increased accuracy.

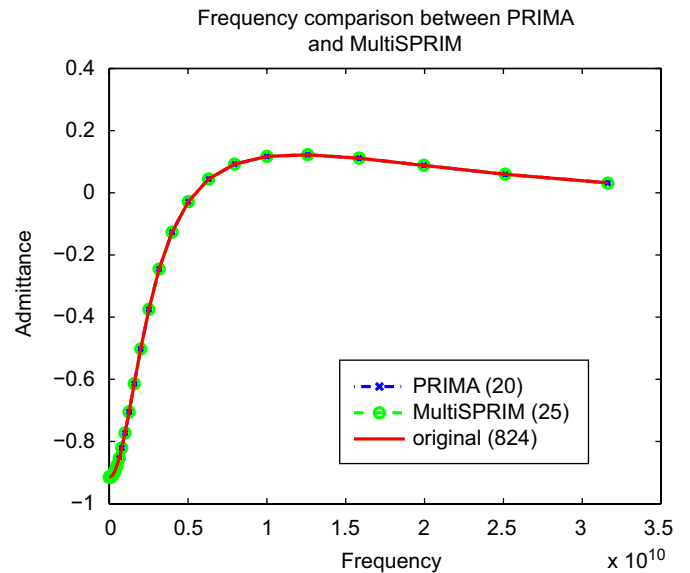


Fig. 7. Accuracy comparison of frequency responses between PRIMA and BSPRIM on the circuit with 824 nodes on y_{12} , (2×2 partitions).

6. Conclusion

In this paper, we have proposed a generalized multi-block structure-preserving reduced-order interconnect macromodeling method (BSPRIM). Theoretically we show how the SPRIM-like structure-preserving MOR method can be extended to deal with RLC circuit matrices in admittance form so that $2q$ moment matching and symmetry are all preserved. We also improve SPRIM by introducing the re-orthonormalization process on the partitioned projection matrix. The proposed BSPRIM method can deal with more circuit partitions, and still match the $2q$ moments and preserve the circuit structure properties like symmetry as SPRIM does. We also show that by increasing partitioning number,

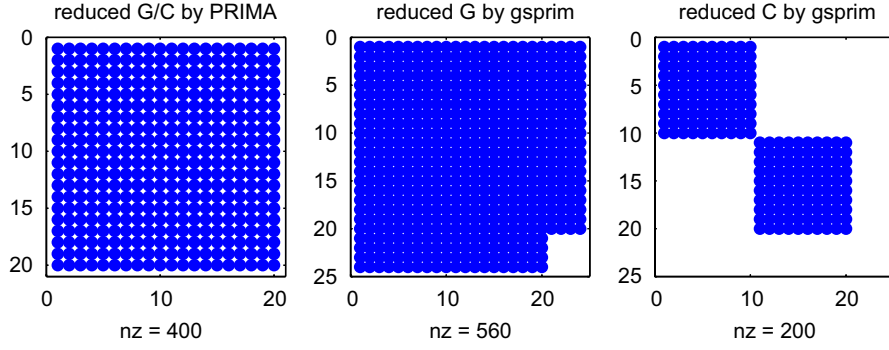


Fig. 8. The structures of the reduced matrices by PRIMA and BSPRIM on the circuit with 824 nodes (2×2 partitions).

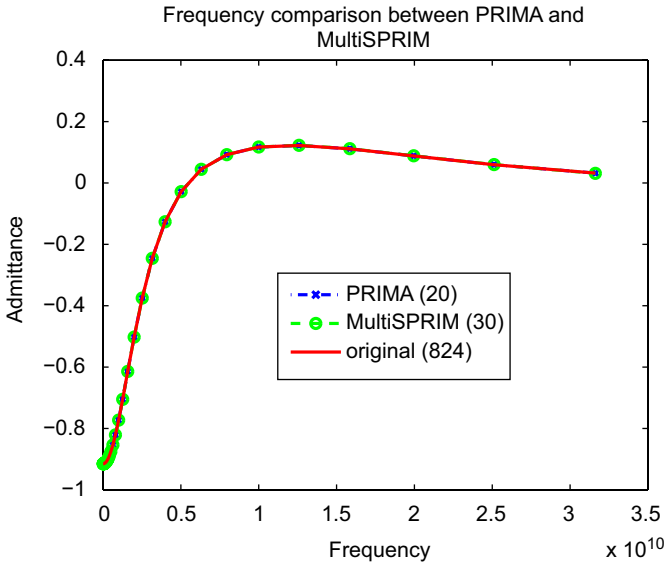


Fig. 9. The accuracy comparison of frequency responses between PRIMA and BSPRIM on the circuit with 824 nodes on y_{12} (4×4 partitions).

BSPRIM can simply build more accurate models, which is more efficient to increase the model accuracy than traditional projection based methods. Experimental results have showed that the BSPRIM outperforms SPRIM in terms of accuracy with more partitions and outperforms PRIMA with less CPU times for generating the same accurate models.

Appendix

Proof of Theorem 1. Our proof basically follows the proof in [1], if we expand in the s_0 , we need to show that the moment from the exact admittance function $Y(s)$ and the reduced one $\tilde{Y}(s)$ match to the $2q$ moment. That is

$$\mathcal{B}^T \mathcal{A}^j \mathcal{R}(s - s_0)^j = \tilde{\mathcal{B}}^T \tilde{\mathcal{A}}^j \tilde{\mathcal{R}}(s - s_0)^j, \quad j = 0, \dots, 2q - 1, \quad (37)$$

where $\mathcal{A} = (\mathcal{G} + s_0 \mathcal{C})^{-1} \mathcal{C}$ and $\mathcal{R} = (\mathcal{G} + s_0 \mathcal{C})^{-1} \mathcal{B}$ and $\tilde{\mathcal{A}} = (\tilde{\mathcal{G}} + s_0 \tilde{\mathcal{C}})^{-1} \tilde{\mathcal{C}}$ and $\tilde{\mathcal{R}} = (\tilde{\mathcal{G}} + s_0 \tilde{\mathcal{C}})^{-1} \tilde{\mathcal{B}}$

As a result, one needs to prove:

$$\mathcal{B}^T \mathcal{A}^{j_1} \tilde{V} = \tilde{\mathcal{B}}^T \tilde{\mathcal{A}}^{j_1}, \quad j_1 = 0, 1, \dots, q, \quad (38)$$

and the following equation, which forms the basic moment theorem [15]:

$$\mathcal{A}^{j_2} \mathcal{R} = \tilde{V} \tilde{\mathcal{A}}^{j_2} \tilde{\mathcal{R}}, \quad j_2 = 0, 1, \dots, q - 1. \quad (39)$$

By combining (38) and (39), we can have (37). So we mainly need to prove (38). Toward this line, we set

$$\mathcal{J} = \mathcal{J}^{-1} = \begin{bmatrix} I_1 & 0 \\ 0 & -I_2 \end{bmatrix}, \quad (40)$$

and I_1, I_2 are identity matrices of the size of the diagonal blocks of \mathcal{C} . So, we have the following relations:

$$\mathcal{G}^T = \mathcal{J}^{-1} \mathcal{G} \mathcal{J}, \quad \mathcal{C} = \mathcal{J}^{-1} \mathcal{C} \mathcal{J}, \quad \mathcal{B} = -\mathcal{J} \mathcal{B}. \quad (41)$$

From these relations, we obtain:

$$(\mathcal{A}^T)^{j_1} = \mathcal{J}^{-1} (\mathcal{C} (\mathcal{G} + s_0 \mathcal{C})^{-1})^{j_1} \mathcal{J}. \quad (42)$$

Since the matrix $\tilde{\mathcal{G}}, \tilde{\mathcal{C}},$ and $\tilde{\mathcal{B}}$ have the same structure as $\mathcal{G}, \mathcal{C},$ and \mathcal{B} , the reduced-order matrices still have

$$\begin{aligned} \tilde{\mathcal{G}}^T &= \tilde{\mathcal{J}}^{-1} \tilde{\mathcal{G}} \tilde{\mathcal{J}}, \quad \tilde{\mathcal{C}} = \tilde{\mathcal{J}}^{-1} \tilde{\mathcal{C}} \tilde{\mathcal{J}}, \quad \tilde{\mathcal{B}} = -\tilde{\mathcal{J}} \tilde{\mathcal{B}}, \\ (\tilde{\mathcal{A}}^T)^{j_1} &= \tilde{\mathcal{J}}^{-1} (\tilde{\mathcal{C}} (\tilde{\mathcal{G}} + s_0 \tilde{\mathcal{C}})^{-1})^{j_1} \tilde{\mathcal{J}}. \end{aligned} \quad (43)$$

Combining (41), (42), and (39), we have

$$\begin{aligned} (\mathcal{A}^T)^{j_1} \mathcal{B} &= -\mathcal{J}^{-1} \mathcal{C} \mathcal{A}^{j_1-1} \mathcal{R} \\ &= -\mathcal{J}^{-1} \mathcal{C} \tilde{V} \tilde{\mathcal{A}}^{j_1-1} (\tilde{\mathcal{G}} + s_0 \tilde{\mathcal{C}})^{-1} \tilde{\mathcal{B}}. \end{aligned} \quad (44)$$

Transposing of Eq. (44) and multiplying at right by \tilde{V} , we can get Eq. (38).

$$\begin{aligned} \mathcal{B}^T \mathcal{A}^{j_1} \tilde{V} &= \tilde{\mathcal{B}}^T \tilde{\mathcal{A}}^{j_1-1} \tilde{\mathcal{J}} (\tilde{\mathcal{C}} (\tilde{\mathcal{G}} + s_0 \tilde{\mathcal{C}})^{-1})^T \tilde{\mathcal{J}} \\ &= \tilde{\mathcal{B}}^T \tilde{\mathcal{A}}^{j_1}. \end{aligned} \quad (45)$$

The proof is complete. \square

Proof of Theorem 2. The difference here from the proof of Theorem 1 is that

$$\mathcal{J}_g = \mathcal{J}_g^{-1} = \begin{bmatrix} I_1 & 0 & \dots & 0 \\ 0 & \ddots & \dots & 0 \\ \vdots & \vdots & I_m & 0 \\ 0 & \dots & 0 & -I_{m+1} \end{bmatrix}. \quad (46)$$

Here, I_1, I_2, \dots, I_m are identity matrices with the same size of V_1, V_2, \dots, V_m . While I_{m+1} is also identity matrix with the same row as V_{m+1} . Then, we have

$$\begin{aligned} \mathcal{G}^T &= \mathcal{J}_g^{-1} \mathcal{G} \mathcal{J}_g, \quad \mathcal{C} = \mathcal{J}_g^{-1} \mathcal{C} \mathcal{J}_g, \quad \mathcal{B} = \mathcal{J}_g \mathcal{B}, \\ (\mathcal{A}^T)^{j_1} &= \mathcal{J}_g^{-1} (\mathcal{C} (\mathcal{G} + s_0 \mathcal{C})^{-1})^{j_1} \mathcal{J}_g. \end{aligned} \quad (47)$$

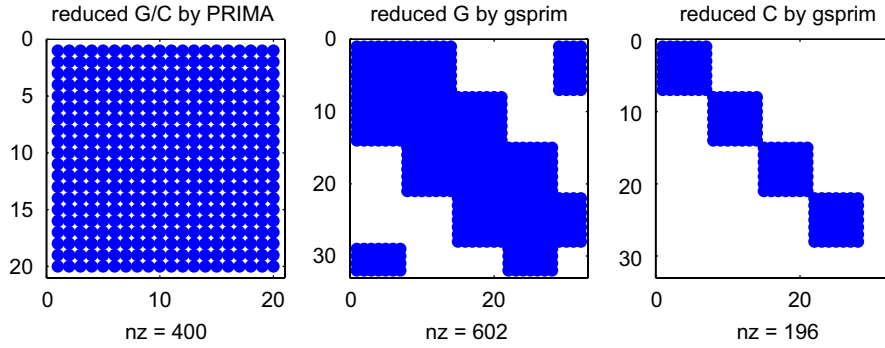


Fig. 10. Structures of the reduced matrices of PRIMA and MultisPRIM on the circuit with 824 nodes (4 × 4 partitions).

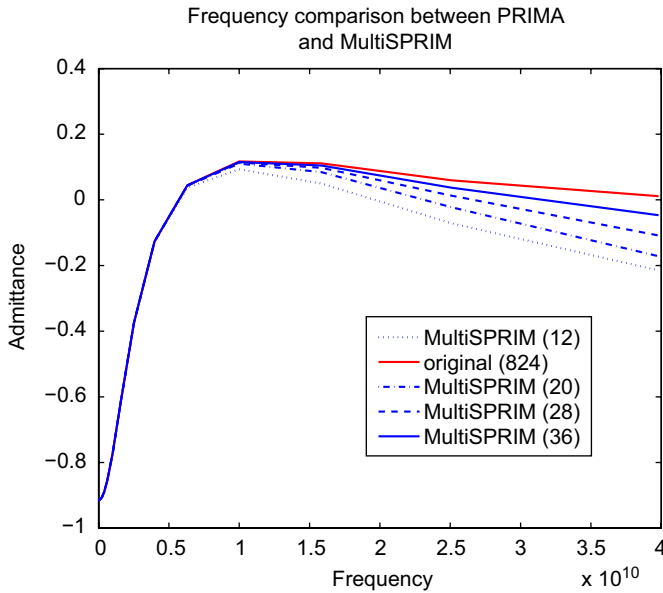


Fig. 11. Frequency responses of y_{12} in the reduced models with different partitioning numbers.

Because of the structure-preserving property of BSPRIM, we can also get the same property of $\hat{\mathcal{G}}$, $\hat{\mathcal{C}}$, and $\hat{\mathcal{B}}$ as in (47).

$$\begin{aligned} \hat{\mathcal{G}}^T &= \hat{\mathcal{J}}_g^{-1} \hat{\mathcal{G}} \hat{\mathcal{J}}_g, & \hat{\mathcal{C}} &= \hat{\mathcal{J}}_g^{-1} \hat{\mathcal{C}} \hat{\mathcal{J}}_g, & \hat{\mathcal{B}} &= -\hat{\mathcal{J}}_g \hat{\mathcal{B}}, \\ (\hat{\mathcal{A}}^T)^j_1 &= \hat{\mathcal{J}}_g^{-1} (\hat{\mathcal{C}}(\hat{\mathcal{G}} + s_0 \hat{\mathcal{C}})^{-1})^j_1 \hat{\mathcal{J}}_g. \end{aligned} \quad (48)$$

The following step is similar in the proof of Theory 1. After we get

$$(\hat{\mathcal{A}}^T)^j_1 \hat{\mathcal{B}} = \hat{\mathcal{J}}_g^{-1} \hat{\mathcal{C}} \tilde{\mathcal{V}}^j_1 (\hat{\mathcal{G}} + s_0 \hat{\mathcal{C}})^{-1} \tilde{\mathcal{B}} \quad (49)$$

we transpose and multiply the result from the right by $\hat{\mathcal{V}}$, we will get

$$\begin{aligned} \hat{\mathcal{B}}^T (\hat{\mathcal{A}}^T)^j_1 \hat{\mathcal{V}} &= \hat{\mathcal{B}}^T \hat{\mathcal{A}}^{j-1}_1 \hat{\mathcal{J}}_g (\hat{\mathcal{C}}(\hat{\mathcal{G}} + s_0 \hat{\mathcal{C}})^{-1})^T \hat{\mathcal{J}}_g \\ &= \hat{\mathcal{B}}^T \hat{\mathcal{A}}^j_1. \end{aligned} \quad (50)$$

The proof is complete. \square

References

[1] R.W. Freund, SPRIM: structure-preserving reduced-order interconnect macro-modeling, in: Proceedings of International Conference on Computer Aided Design (ICCAD), 2004, pp. 80–87.
 [2] N. Mi, B. Yuan, S.X.-D. Tan, H. Yu, General block structure-preserving reduced order modeling of linear dynamic circuits, in: Proceedings of International Symposium on Quality Electronic Design (ISQED), 2007, pp. 633–638.

[3] J. Lillis, C. Cheng, S. Lin, N. Chang, Interconnect Analysis and Synthesis, Wiley, New York, 1999.
 [4] L.T. Pillage, R.A. Rohrer, Asymptotic waveform evaluation for timing analysis, IEEE Trans. Comput.-Aided Des. Integrated Circuits Syst. (1990) 352–366.
 [5] P. Feldmann, R.W. Freund, Efficient linear circuit analysis by Padé approximation via the Lanczos process, IEEE Trans. Comput.-Aided Des. Integrated Circuits Syst. 14 (5) (1995) 639–649.
 [6] M. Silveira, M. Kamon, I. Elfadel, J. White, A coordinate-transformed Arnoldi algorithm for generating guaranteed stable reduced-order models of RLC circuits, in: Proceedings of International Conference on Computer Aided Design (ICCAD), 1996, pp. 288–294.
 [7] K.J. Kerns, A.T. Yang, Stable and efficient reduction of large, multiport rc network by pole analysis via congruence transformations, IEEE Trans. Comput.-Aided Des. Integrated Circuits Syst. 16 (7) (1998) 734–744.
 [8] A. Odabasioglu, M. Celik, L. Pileggi, PRIMA: passive reduced-order interconnect macromodeling algorithm, IEEE Trans. Comput.-Aided Des. Integrated Circuits Syst. (1998) 645–654.
 [9] S.X.-D. Tan, A general hierarchical circuit modeling and simulation algorithm, IEEE Trans. Comput.-Aided Des. Integrated Circuits Syst. (2005) 418–434.
 [10] S.X.-D. Tan, L. He, Advanced Model Order Reduction Techniques in VLSI Design, Cambridge University Press, Cambridge, 2007.
 [11] Z. Qi, H. Yu, P. Liu, S.X.-D. Tan, L. He, Wideband passive multi-port model order reduction and realization of RLCM circuits, IEEE Trans. Comput.-Aided Des. Integrated Circuits Syst. (2006) 1496–1509.
 [12] H. Yu, L. He, S.X.D. Tan, Block structure preserving model reduction for linear circuits with large numbers of ports, in: Proceedings of IEEE International Workshop on Behavioral Modeling and Simulation (BMAS), 2005, pp. 1–6.
 [13] H. Yu, Y. Shi, L. He, Fast analysis of structured power grid by triangularization based structure preserving model order reduction, in: Proceedings of Design Automation Conference (DAC), 2006, pp. 205–210.
 [14] R. Freund, Padé-type model reduction of second-order and higher-order linear dynamical systems, in: P. Benner, V. Mehrmann, D. Sorensen (Eds.), Dimension Reduction of Large-Scale Systems, Lecture Notes in Computational Science and Engineering, vol. 45, Springer, Berlin, 2005, pp. 191–223.
 [15] E.J. Grimme, Krylov projection methods for model reduction, Ph.D. Thesis, University of Illinois at Urbana-Champaign, 1997.



Ning Mi (S'05) received the B.S. degree in electrical engineering from the Peking University, Beijing, China in 2005 and the M.S. degree in electrical engineering from University of California, Riverside, in 2007. She is currently a Ph.D. candidate in electrical engineering from University of California, Riverside. Her research interests include power grid analysis and model order reduction considering process variations.



Sheldon X.-D. Tan (S'96–M'99–SM'06) received his B.S. and M.S. degrees in electrical engineering from Fudan University, Shanghai, China in 1992 and 1995, respectively and the Ph.D. degree in electrical and computer engineering from the University of Iowa, Iowa City, in 1999.

He is an Associate Professor in the Department of Electrical Engineering, University of California, Riverside. He was a faculty member in the Electrical Engineering Department of Fudan University from 1995 to 1996. His research interests include several aspects of design automation for VLSI integrated circuits — modeling and simulation of analog/RF/

mixed-signal VLSI circuits, high-performance power and clock distribution network simulation and design, signal integrity, power modeling, thermal modeling, thermal optimization in VLSI physical and architecture levels and embedded system designs based on FPGA platforms.

Dr. Tan is the recipient of NSF CAREER Award in 2004. Dr. Tan received a Best Paper Award from 2007 International Conference on Computer Design (ICCD'07), Best Paper Award Nomination from 2005 IEEE/ACM Design Automation Conference, Best Paper Award from 1999 IEEE/ACM Design Automation Conference and the Best Poster Award from 1999 Spring Meeting of the NSF Center for Design of Analog and Digital Integrated Circuits (CDADIC). He also co-authored the book "Symbolic Analysis and Reduction of VLSI Circuits" by Springer/Kluwer 2005. He is an associate editor for Journal of VLSI Design and served as a technical program committee member for ASPDAC, BMAS, ASPDAC, ISQED, and ICCAD.



Boyuan Yan (S'05) received the B.S. degree in electrical engineering from Dalian University of Technology, Dalian, China, in 2004, and the M.S. degree in electrical engineering, in 2007, from the University of California, Riverside, where he is currently working toward the Ph.D. degree. His research interests include model order reduction of large-scale circuits and systems.